Published in final edited form as:
Int J Radiat Biol. 2014 September ; 90(9): 799–806. doi:10.3109/09553002.2014.938278.

Radiation induced cognitive impairment and altered diffusion tensor imaging in a juvenile rat model of cranial radiotherapy

Ann M. Peiffer[1,4], **Rebecca M. Creer**[2], **Constance Linville**[1], **John Olson**[3], **Praveen Kulkarni**[5], **Jacquelyn Ann Brown**[1], **David R. Riddle**[2,4], **Mike E. Robbins**[1,4,†], and **Judy E. Brunso-Bechtold**[2,4]

[1]Department of Radiation Oncology, Wake Forest School of Medicine, Winston-Salem, NC 27157

[2]Department of Neurobiology and Anatomy, Wake Forest School of Medicine, Winston-Salem, NC 27157

[3]Center for Biomolecular Imaging, Wake Forest School of Medicine, Winston-Salem, NC 27157

[4]Brain Tumor Center of Excellence, Wake Forest School of Medicine, Winston-Salem, NC 27157

[5]Center for Translational NeuroImaging, Northeastern University, Boston, MA 02115

Abstract

Purpose—Assess the long term effects of fractionated whole brain irradiation (fWBI) using diffusion tensor imaging (DTI) and behavior in a pediatric rodent model for the clinical presentation of adult pediatric cancer survivors.

Materials and Methods—Five week old, male F344xBN rats were randomized to receive 0, 5, or 6.5 Gy fractions biweekly for 3 weeks, resulting in Sham, Irradiated-30 (IR-30) and IR-39 Gy total dose groups. Magnetic Resonance Imaging occurred at 1, 3, 6 and 9 months with behavioral assessment at 10–11 months post-fWBI.

Results—Irradiation reduced brain size ($p<0.001$) and body weight ($p<0.001$) proportionate to dose. At 1 month post-fWBI and throughout follow-up, diffusion was reduced in IR-30 and IR-39 relative to shams ($p<0.001$). IR-30 but not IR-39 rats were impaired relative to Shams on the

Corresponding Author: Ann M. Peiffer, PhD, Wake Forest School of Medicine, Dept. of Radiation Oncology Medical Center Blvd., Winston-Salem, NC 25157apeiffer@wakehealth.eduPhone: 1-336-713-6535 Fax: 1-366-713-6565.
†Deceased

Declaration of Interest: No other conflicts of interest to report.

reversal trial of the Morris Water Maze ($p<0.05$), and IR-30 rats preferred a striatum-mediated strategy ($p<0.06$).

Conclusions—Hippocampal performance was impaired in IR-30 but not IR-39 animals. While gross size differences exist, white matter integrity is preserved in rats after fWBI at 5 weeks. This significant departure from childhood cancer survivors and single fraction rodent studies where white matter degradation is a prominent feature are discussed.

Keywords

Rat; Brain; MRI; Pediatric; fractionated whole-brain irradiation

Introduction

Biological response has been noted to vary among patients of different age groups with younger patients often experiencing more severe late effects related to radiotherapy. The relationship between development and aging interplay with many diseases, including cancer, to produce vast differences in the occurrence, presentation, response to treatment, and outcome of the disease (Haffty and Wilson, 2007). For example, the type and location of many central nervous system (CNS) tumors is known to change over a lifespan; specifically, posterior germ-cell tumors are more common in pediatric patients whereas more anterior, non-germ cell tumors are more common in adults. Selecting a proper treatment modality (e.g., surgery, chemo, radiation therapy, or combination) depends on several factors, including the location of disease, historical survival with the proposed treatment, and the impact of treatment on quality of life. Optimizing treatment(s) to optimize survival and minimize negative impact on quality of life has become an important endpoint in many clinical trials (Harrop et al., 2011). Chemotherapy is often the preferred treatment for younger children with cancer since radiotherapy (RT) is known to produce impairments in cognition that tend to be more severe than those seen with chemotherapy. However, due to the difficulty seen with therapies failing to cross the blood brain barrier and the lack of response in some brain tumors to chemotherapeutic agents, radiation therapy is still used to treat many childhood cancers.

According to the American Cancer Society's 2014 Facts and Figures, 10,450 new cancer cases among children 0–14 years of age are expected in 2014 (American Cancer Society, 2014). Malignant cancers of the brain and nervous system represent the second largest group of childhood malignancies, at 21% of cases across all races. Even though childhood mortality rates for cancer have declined by 53% since 1975, cancer remains the second leading cause of death in children (Jemal et al., 2011). Due to improved treatment regimens, survival rates have increased and a larger proportion of childhood cancer survivors are living longer (e.g., 5 year survival for brain and other nervous system cancers diagnosed in 1975–1979 was 59% vs.75% for cases diagnosed between 2003–2009) (American Cancer Society, 2014). Of the estimated 379,112 survivors of childhood cancer (diagnosed at 0–19 years of age) alive in the United States of America (USA) as of 2010, 59,083 or 15.6% survived brain and nervous system primaries (American Cancer Society, 2014). Those treatments, however, carry with them risks for side effects that can often significantly impair the quality of life of these children as they mature. This dilemma has prompted the Children's

Oncology Group (COG) to develop and implement longterm follow-up guidelines for screening and management of late effects (e.g., cognitive function, secondary cancers, etc.) in survivors of childhood cancer (Landier et al., 2004).

With the increased importance of long-term impact of treatment therapies on cognition, it is imperative that model animal systems be assessed for cognitive outcomes longitudinally and at late time points. To assess radioprotective agents, clear behavioral studies with measures sensitive to irradiation will also need to be identified. In addition, due to the known differences in the biological response to fractionated irradiation protocols, animal models intended to inform us of the human condition in clinical treatments should use a fractionated regimen instead of single-dose treatments (see for example (Gaber et al., 2003, Yuan et al., 2006) and Greene-Schloesser et al. this issue). Specifically in reference to white matter hyperintensity development, to our knowledge, there has been no fractionated regimen in a model rodent system to date, that has shown long-term effects in white matter disease. Rather, single-dose studies have been shown to produce white matter hyperintensities and necrosis (e.g., (Wang et al., 2009, Chan et al., 2009)). Here we present the functional and structural impact of fractionated irradiation at 30 or 39 Gy in F334xBN rat pups beginning at 5 weeks of age, an age that best corresponds to early adolescence in humans (Kolb et al., 2012). We hypothesized that i) juvenile rats receiving fWBI would show impaired cognitive abilities and altered neural microstructure, especially within white matter tracts, and ii) that radiation-induced changes would be greater in rats treated with 39 Gy fWBI than in rats treated with 30 Gy.

Materials and Methods

Subjects

Male F344xBN rats (N=36, Harlan Industries, Indianapolis, Indiana, USA) were received at 3 weeks of age and randomly assigned to one of 3 conditions - sham irradiated controls (Sham), 30 Gy fWBI (IR-30) or 39 Gy fWBI (IR-39). The longitudinal study time line is shown in Figure 1. Beginning at 5 weeks of age, fWBI rats were anesthetized (26.5 mg/kg ketamine, 5.4 mg/kg xylazine) and irradiated in a self-shielded 137Cs irradiator using lead and Cerrobend shielding devices to collimate the beam so that the whole brain was irradiated. For IR-30 rats, a total dose of 30 Gy was delivered to the brain as 6 fractions of 5 Gy, twice per week for 3 weeks. In IR-39 rats, this scheme was modified by giving 6.5 Gy/fraction to achieve a total dose of 39 Gy. Biological effective dose (BED) calculations ($\alpha/\beta=3$) place these dose schedules at 80 and 123.5 Gy. For comparison, a pediatric total dose of 50.4Gy at a 1.8Gy/fraction dose schedule has a BED of 80.6Gy. Each dose was delivered to alternate sides of the head on alternate days to ensure that each rat received the same midline dose. Sham rats were anesthetized, but not irradiated. The animal protocol for this study conformed to National Institutes of Health guidelines and was approved by the Animal Care and Use Committee of Wake Forest University Health Sciences. Rats were pair-housed in a climate-controlled environment with a 12-hour light/dark cycle and provided food and water ad libitum. When tooth care was required, the entire cohort was anesthetized.

Magnetic Resonance (MR) Imaging

All MR imaging was performed in a Bruker Biospec 7.0 Tesla 30 cm I.D. horizontal bore magnet (Bruker Biospin; Ettlingen, Germany) equipped with a Bruker S116 actively shielded gradient coil. A 38mm linear quadrature Litzcage Radio Frequency (RF) transceiver volume coil (Doty Scientific; Columbia, South Carolina, USA), tuned to 300.2MHz was used for signal transmission and reception. A Linux workstation running ParaVision 4.0 interfaced the user with the scanner. Anesthesia was induced with isoflurane (3%) and oxygen (4 L/min) in an induction chamber (Surgivet; Waukesha, Wisconsin, USA). Once anesthesia was induced, isoflurane and oxygen flow to the rat were reduced (1.5% and 1 L/min) and maintained via an MR compatible nose cone. The rat's respiration and body temperature were monitored throughout the scan (SAI Instruments; Stony Brook, New York, USA). Respiration was maintained between 35 and 45 breaths per minute by adjusting isoflurane levels. Body temperature was maintained at 37°C by blowing thermostatically controlled warm air into the bore of the magnet.

Each animal was positioned with the brain in the isocenter of the magnet and RF coil. A three plane localizer scan [Rapid Acquisition with Relaxation Enhancement (RARE) pulse sequence with parameters: Repetition Time (TR) = 1500ms, Echo Time (TE) = 30ms, Field of View (FOV) = 3.5cm, slice thickness = 2mm, matrix = 256×256, number of averages (NEX) = 1] was acquired and used to precisely center the animal's brain in the system. Once the animal was correctly positioned, a set of high resolution sagittal T2-weighted structural images were acquired, using a RARE pulse sequence with parameters: TR = 6600ms, TE = 60ms, FOV = 3.0cm, slice thickness = 0.5mm, matrix = 256×256, NEX = 6. Animals were imaged 1, 3, 6 and 9 months (approximately 12, 20, 32 and 62 weeks of age) post-irradiation (post-IR). Utilizing ImageJ (http://rsb.info.nih.gov/ij/index.html), total brain volume was calculated at 9 months by delineating neural tissue on each animal's T2-weighted image by CL, who was blinded to condition.

Diffusion Tensor Imaging (DTI)

A 2-shot 2 dimensional spin-echo, echo planar imaging (EPI) pulse sequence was used to acquire DTI data. A slab of 20 contiguous coronal slices through the forebrain was positioned using the high resolution T2-weighted images. The EPI slice package was positioned so that the 9^{th} slice of 20 (slice number 12, see Figure 2A) was centered on the anterior commissure. The EPI DTI parameters were: TR=3000ms, TE=37.8ms, FOV=4.0cm, matrix=128×128 (in-plane resolution = 313μm), slice thickness = 620μm, diffusion gradient duration (d) = 4ms, diffusion gradient separation (D) = 20ms, b-max = 2924s/mm2 in 30 noncolinear directions (with 5 b0 images acquired) and 8 averages. EPI images were converted to compressed nifti format using MRIcron (http://www.sph.sc.edu/comd/rorden/mricron/dcm2nii.html).

DTI Data Processing

Using MedINRIA 1.9.2 (http://wwwsop.inria.fr/asclepios/software/MedINRIA/), fractional anisotropy (FA), the three eigenvalues (λ1, λ2, and λ3) and Trace (summed diffusion across eigenvalues) were obtained from the data. After removal of posterior slices too degraded by imaging artifacts, images were manually aligned as described in (Ferris et al., 2005) to a

template containing 158 pre-defined regions of interest (ROI) using rigid-body transforms by JK who was blind to treatment condition (see Figure 2B for an example of a registration). Visual inspection confirmed good alignment and lack of registration errors for the ROI of interest. Following alignment, the mean, standard deviation and number of voxels were assessed for 5 pre-defined areas of interest: 1) frontal cortex (i.e., anterior cingulate, anterior olfactory nucleus, infralimbic cortex, prelimbic cortex, and tenia tecta); 2) dentate gyrus (DG); 3) dorsal cornus ammonis (CA) 1 and CA3 of hippocampus; 4) striatum (i.e., dorsal medial and lateral, ventral medial and lateral) and 5) white matter (cingulum, corpus callosum and deep cortical white matter also known as external capsule). White matter integrity was evaluated using FA and diffusion parameters within the white matter ROI. For frontal cortex, striatum and hippocampal ROI diffusion parameters represent a mix of tissue classes and therefore differences could not be attributed to white matter integrity. Rather for these ROI, diffusion parameters indicate microstructural tissue parameters. SPSS v18.0 was used to assess these values and determine if differences between conditions existed and if these anatomical markers related to behavioral performance measures. Repeated measure analysis was adjusted using the Greenhouse-Geisser correction for sphericity. F-statistic values are listed with the degrees of freedom of the analysis listed as the subscript (e.g., $F_{2,27}$)

Behavioral Assessments

Behavioral assessment began at month 10 post-irradiation following the last imaging session.

Morris Water Maze (MWM) is a standard assessment of spatial learning ability. The maze consisted of a circular pool (1.83 m diameter and 0.58 m height) with an escape platform centered in one of the four maze quadrants. Rats were trained over 12 days (4 blocks of training with 6 trials, 2 trials/day) to locate an escape platform hidden just below the water surface. There were two types of trials, training trials and probe trials. During a training trial (5 per block), the animal was allowed to swim for 90 seconds (s) to locate the platform. Every sixth trial a 30 s probe trial assessed the development of a spatially localized search for the escape platform.

During the probe trial, the platform was made unavailable for escape. The accuracy of the search for the platform location was measured by the proximity to the escape location for 30 s with the subject's position sampled ten times/s and summed. There were four interpolated probe trials, the sum of which was used to generate a composite score. Lower proximity scores represent a more accurate search and better spatial learning of the platform location.

Delayed Match to Place (DMP) was based on a protocol published by Steele and Morris (1999) and delivered with specific modifications to reflect the overall protocol of this experiment. Rats were tested using a unique daily platform location and 4 trials/day. Rats had 90 s to locate the platform, were led to the escape platform if time elapsed, and had a 20 min delay between trial 1 and 2 with 15 s delays between all other trials. Day 1 was designed as a reversal with the platform now located in the opposite quadrant from the MWM. Day 2 and 3 had locations in the other 2 quadrants and in the outer and inner annulus, respectively. On Day 4, the platform returned to the standard MWM location to

reinforce this position for later testing. A Savings score was calculated by taking the difference in escape latency between trial 1 and 2. Higher positive Savings values indicated better memory of the new platform location.

Visual Acuity testing occurred on day 19 of MWM testing following a two-day break and assessed sensorimotor and motivational factors independent of spatial learning. Cue training to a visible escape platform consisted of four sequential trials. Rats started in the center of one quadrant and visible platform locations were randomized in the center of the other three quadrants. Path length, distance to platform, swim velocity, and escape latency was assessed for outliers and significant differences between treatment groups that could influence performance aside from spatial learning ability.

Strategy Preference was then assessed and evaluated as outlined in the work of Nicolle and colleagues (2003) and consisted of 2 days of training trials with a submerged escape platform in accordance with the standard MWM protocol above. Two trials were performed each day with a 3 hour inter-trial interval. On day 3, two 90 s probe trials were administered. Probe trials consisted of a visible platform placed opposite to the standard MWM location. Rats entered the arena facing the wall perpendicular to the platform plane. A “place” strategy was recorded if the rat crossed a 40 cm perimeter centered on the standard hidden platform location (i.e., training trial location) prior to mounting the visible platform. If the rat went to the visible platform without crossing this perimeter a “cue” strategy was recorded.

Tissue Processing

At 12 months post-irradiation, animals were deeply anesthetized with sodium pentobarbital (150 mg/kg body weight, Ovation Pharmaceuticals, Inc.; Deerfield, IL) and then decapitated. The brain was removed and chilled for 3 minutes in cold artificial cerebrospinal fluid (140mM NaCl, 5mM KCl, 1mM $MgCl_2$, 1mM $CaCl_2$, 24mM dextrose, 10mM HEPES, pH 7.4). Pituitaries were collected immediately following brain removal. The brain was then bisected along midline and the left hemisphere was immersion fixed for future histology and analyses. The right hemisphere was then cut in the coronal plane at the optic chiasm. From the rostral portion, striatum was removed leaving frontal cortex. From the caudal portion, hippocampus was dissected and the remaining cortex was cut in half at the rhinal fissure (anterior portion labeled dorsal cortex and the other the ventral cortex). All tissue samples were weighed in 0.5 ml microtubes, frozen on dry ice, and stored at −80°C.

Results

Subjects

Six animals (16.7%) died during the three weeks of irradiation (3 Sham, 1 IR-30 and 2 IR-39) most likely from complications with anesthesia, resulting in 9 Sham, 11 IR-30 and 10 IR-39 available for analysis. One additional IR-30 subject died from undeterminable causes following the last DTI and prior to behavioral testing; thus all measured behavioral results were from 9 Sham, 10 IR-30 and 10 IR-39. General irradiation effects were evident on body weight ($F_{2,26}$=120.26, $p<0.001$) and teeth condition. Weight was monitored throughout the

study and remained consistent over the 7 weeks between the final imaging session, behavioral tests and sacrifice. During this 7 week period a dose dependent response was seen; sham animals (mean 483.51g) were significantly ($p<0.001$) heavier than IR-30 rats (mean 350.39g) that were significantly ($p<0.01$) heavier than IR-39 (mean 319.84g) rats. A significant difference in the number of teeth clippings required between the treatment groups was observed over the entire period post-IR as well. In part, this difference could have resulted from primary effects of irradiation to the developing teeth or due to the inability of IR-39 rats and a delay of 60–152 days for IR-30 rats to return to hard food following irradiation. Sham animals never required teeth clipping while IR-30 animals needed an average of 4 clippings and IR-39 needed an average of 19 clippings per animal. Again, at each teeth clipping all animals in the cohort were anesthetized to keep the anesthesia effect equivalent across the treatment groups.

MRI Measures

Total Brain Volume—A main effect of irradiation was seen for total brain volume 9 months post-irradiation ($F_{2,27}=139.56$, $p<0.001$); Sham rats had significantly larger brains (mean 2161.36mm^3 +/− 13.22) than either irradiation group ($p<0.001$). IR-30 rats had significantly larger brains (mean 1953.68mm^3 +/−40.09) than IR-39 rats (mean 1906.25mm^3 +/−7.30, $p<0.01$).

General Diffusion—Across all regions and time points, irradiation reduced Trace measures of diffusion in both IR-30 and IR-39 relative to Sham rats (see white matter ROI data in Figure 3A). Condition was significant ($p<0.02$) and post-hoc analysis showed significant differences between Sham and both irradiated groups ($p<0.01$) for all ROI except Dentate, where IR-39 but not IR-30 rats ($p<0.4$) were significantly different from Shams. IR-39 rats showed less diffusion than IR-30 ($p<0.05$) for all ROI except Dentate where a marginal decrease ($p=0.054$) was seen. Time showed a significant linear decrease in Trace for all ROI across the 4 time points following irradiation. This decrease did not significantly interact with Condition. Individual eigenvalues ($\lambda 1$–3) were similarly distributed to Trace values. A few exceptions were seen, including a significant Time×Condition interaction for $\lambda 1$ values in the Frontal ROI ($F_{4.4,58.8}=4.02$, $p<0.01$) that was driven by a larger decrease in $\lambda 1$ for IR-30 rats at 3 months post-IR than IR-39 rats. Post-hoc analysis of the significant Condition effect failed to see differences between IR-30 and 39 rats for $\lambda 2/3$ in white matter and $\lambda 1$ for Dentate.

Directional Diffusion—Fractional Anisotropy (FA) did not differ by condition in white matter (Figure 3B) nor any ROI except for Dorsal CA1 and CA3 ($F_{2,27}=4.37$, $p<0.03$). In Dorsal CA1 and CA3 ROI, Sham rats showed significantly lower FA than IR-39 rats ($p<0.02$) but not IR-30 rats ($p<0.3$). Irradiated rats failed to differ from each other ($p<0.2$). Time showed a significant effect indicative of linear decreases in FA across all ROI ($p<0.01$) except Dentate ($p<0.3$). Time decreases did not significantly interact with Condition except for the Frontal FA ROI ($F_{4.4,59.0}=2.57$, $p<0.05$) where Sham rats showed significantly less FA than irradiated groups at the 9th month post-IR scan ($p<0.001$) but at previous scans showed no significant differences.

Behavioral Assessments

Visual Acuity—All comparisons showed no significant differences among conditions ($F_{2,26}<1$) and no rat was found to suffer from gross disparities in ability to find a visible platform or swim.

Standard MWM—Across Blocks and Trials, learning improved and reached asymptotic levels in all 3 experimental groups. Distance to platform, escape latency and path length, did not significantly differ or interact with condition. A significant Condition effect ($F_{2,27}=3.65$, $p<0.05$) was found on swim velocity with IR-30 rats swimming significantly faster than Sham or IR-39 rats (24.75 cm/s vs. 22.82 and 23.10, respectively). For Probe trials, improvement was seen across Blocks for distance to platform, time over platform location, and percent of time in platform zone. Again, these variables did not significantly differ nor interact with Condition. In regards to swim velocity on probe trials, no significant difference was seen among Conditions or across Blocks.

DMP—Day 1 was a reversal of the standard MWM platform location and revealed a significant Condition effect ($F_{2,26}=3.61$, $p<0.05$) in Savings between Trial 1 and 2 (see Figure 4A). IR-30 rats failed to recall the new platform location and did not improve their time in Trial 2, resulting in an average Savings of -12.8 +/−8.73. IR-30 rats performed significantly worse ($p<0.05$) relative to Sham (27.81 +/−17.44) and IR-39 rats (35.78 +/−16.48), who did not differ significantly from each other. While results remained trends over the 4 days of testing, they were not significant in the overall analysis due to the large degree of variability. The difference between Sham and IR-30 rats remained marginally significant ($p<0.06$; see Figure 4B). Condition did not show a main effect or interaction with escape latency, mean distance to platform or percent time in previous platform zone which all showed improved performance across Days and Trials.

Strategy Preference—A spatial/place strategy, which involves the flexible use of spatial cues, is dependent upon intact hippocampal circuitry. Conversely, a response/cue strategy, or the formation of associations between discrete cues and behavioral responses, is dependent upon intact striatal circuitry. As expected, equal numbers of Sham rats operated with a place or cue strategy (see Table I). IR-30 rats, however, tended to prefer a cue rather than place strategy ($p<0.06$); whereas IR-39 rats were similar to Sham animals and showed no preference. It is important to note that performance on the 4 trials prior to the strategy probe trial mirrored performance during the final block of standard MWM and indicated that the spatial value of the escape platform location had not been altered substantially with the DMP and Visual Acuity tests. Further, since this is a single trial test, results should be interpreted cautiously; however they independently confirm the DMP difference seen on the reversal day.

Gross Brain Morphology

Similar to our work in older rats, no white matter necrosis was visually observed at dissection. Overall, Condition had a significant impact on brain weight of the right hemisphere ($F_{2,25}=16.47$, $p<0.001$), with sham greater than either irradiated group ($p<0.01$) and IR-30 greater than IR-39 rats ($p<0.05$). Condition and Brain Subdivision significantly

interacted ($F_{10,125}$=3.99, p<0.01), and further analyses addressed which subdivisions were significantly different. Sham animals differed significantly from the irradiated groups in the weight of the pituitary ($F_{2,25}$=8.10, p<0.01), hippocampus ($F_{2,25}$=9.11, p<0.001) and ventral cortex ($F_{2,25}$=12.49, p<0.001) but not in the weight of striatum ($F_{2,25}$ <1), frontal cortex ($F_{2,25}$=1.54, ns) or dorsal cortex ($F_{2,25}$ <1). Post-hoc analysis revealed that shams had significantly heavier pituitaries and ventral cortices than both IR-30 (p<0.01, p<0.03) and IR-39 (p<0.01, p<0.001) rats. For the hippocampus, sham rats were significantly heavier than the IR-39 rats (p<0.001) but not the IR-30 rats (p<0.14). Post-hoc analysis between the irradiated groups indicated no weight differences in pituitary (p<0.7) and ventral cortex (p<0.3) with significantly heavier hippocampus (p<0.03) in IR-30 than IR-39 rats.

Discussion

Fractionated WBI beginning at 5 weeks of age decreased body and brain weight and reduced total brain volume and Trace diffusion rates. Fractional Anisotropy (FA) of the white matter tracts was unaffected by irradiation but decreased with time, presumably due to increasing age. Cognitive testing revealed impairment on the delayed match to place task in rats that received 30 Gy fWBI but not in rats that received 39 Gy. When strategy preference was assessed, rats receiving the lower dose, but not sham control rats or rats receiving the higher dose, appeared to prefer a non-hippocampal strategy in the MWM. The DMP and strategy preference results suggest a radiation-induced functional change in the hippocampal circuit that, paradoxically, was evident in rats treated with 30 Gy fWBI but not in rats treated with 39 Gy. Of interest to this functional difference was the relative lack of DTI findings that 39 Gy rats differed significantly from IR-30 rats, except for the greater decrease in eigenvalue λ1 for the frontal ROI at 3 months post-fWBI. While gross brain and body weight significantly differed between IR-30 and IR-39, it is unclear what biological significance this represents. Future histological analyses are required, especially centered around the 3 month post-fWBI period. At present, these results have intriguing implications for irradiation research utilizing rat models of cognition and call for more dose-response research directed at fractionated rather than single dose methodologies in model animal systems.

In this study, sham rats had greater diffusion than irradiated rats, suggesting that irradiation damage does not appear to replicate diffusion parameters in the appearance of stroke or an advanced aging process, where greater diffusion is related to impaired tissue integrity (i.e., excess fluid in tissues) and predicts poorer function (Chabert and Scifo, 2007, Pierpaoli et al., 1996, Sotak, 2002). The results in the present study indicate the inverse phenomenon, at least in the case of IR-30 rats (less diffusion and poorer function). However, both groups of irradiated animals are smaller in brain volume and body weight compared to sham animals. Reduced body size is most likely due to lack of growth hormone resulting from irradiation injury to the pituitary (see (Molina et al., 2013, Forbes et al., 2013) for discussion) which is greater in the IR-39 group relative to the IR-30 rats. If the irradiated animals had smaller brain volume with the same number of cells, the tissue would have an increased packing density and therefore a smaller amount of diffusion. Pilot stereological inspection of the dentate gyrus did not suggest a dramatic difference in neuronal packing density (NeuN+ staining). However, we cannot rule out a difference in cell density involving neurons and/or

glia. For example, radiation exposure increases the number and production of activated microglia which could in turn increase cell packing density and lower diffusion. Alternatively, radiation exposure may impact extracellular matrix proteins which could impede diffusion separate from cell packing density. Extensive stereological analyses will be required to test for changes in cell density and will be pursued in future studies.

Regardless of cell packing, the largest discrepancy with this fractionated animal model when comparing diffusion to adult survivors of childhood cancer is the lack of white matter change. For adult survivors of childhood cancer, white matter has been observed to have higher diffusion and decreased directionality (i.e. FA) compared to similar aged controls with no history of cancer treatment (Dellani et al., 2008, von der Weid, 2008, Khong et al., 2006). Vulnerability of white matter to irradiation has been shown to be driven by mechanisms including reduced blood flow via vascular damage and less or ill-formed myelin via a reduced oligodendrocytes progenitor pool and increased cytokine expression (as reviewed in (Belka et al., 2001, Greene-Schloesser et al., 2012)). This lack of structural white matter damage is in line with previous work in older animals following this fWBI regimen as evaluated with DTI and extensive histology (i.e., lack of observed white matter necrosis and no irradiation effect for size of the major forebrain commissures, number of oligodendrocytes, size and number of myelinated axons or the thickness of myelin (Peiffer et al., 2010, Shi et al., 2006, Shi et al., 2009, Shi et al., 2008)). Successful rodent models of white matter damage to date have relied on single-dose irradiation that is mechanistically different from fractionated protocols used in the clinic (for examples (Wang et al., 2009, Chan et al., 2009)). Physiologically, white matter is more vascularized and proportionally different in rodents which have only 14% of their cortex in white matter tracts versus 50% in humans (Zhang and Sejnowski, 2000). These differences in individual tissue compartments within the brain make translating findings across species and across irradiation fractionation schemes quite complicated. Another significant difference is the dose rate of irradiation delivered in model animal systems (~2Gy/min in this case) versus ~7Gy/min in the clinic. Hypofractionation will cause more late effect damage at higher dose rates than at lower (Fletcher, 1991), and future fractionated rodent studies with an increased dose rate may enhance the clinical relevance of this model. It may be that the white matter damage is not a direct result of the total dose to the tissue but the more complicated interaction between fractionation, dose per fraction and ability of the tissue type to repair based on blood vessel density.

The results of cognitive testing indicated a deficit partly associated with hippocampal dysfunction in IR-30 rats. Complex cognitive tasks are completed via a prefrontal cortex – hippocampal – striatal axis (see (Moustafa and Gluck, 2011) for review). Each area while connected can be dissociated and shown to contribute unique processing to varying aspects of memory tasks. Prefrontal cortex provides executive function, attention, and stimulus selection properties, while hippocampus processes spatial and stimulus representational learning in declarative memory (Moustafa and Gluck, 2011). Finally, striatum is involved in stimulus response motor learning or implicit memory (Moustafa and Gluck, 2011). Each of these brain regions may have a different functional injury threshold associated with irradiation that impacts how the hippocampus operates as part of the larger cortical circuit. Functional injury across this circuit will need to be assessed directly using

neurophysiological methods to explain why a dose of 30 Gy but not 39 Gy could produce an imbalance leading to impaired reversal performance and preference for a striatum mediated strategy via hippocampal damage. Of note within this circuit, dopamine modulation for patients with Parkinson's disease can lead to both positive and negative consequences for brain plasticity due to alterations in striatal dopamine levels and initial baseline performance (Cools, 2006). To determine whether the difference between IR-30 and 39 rats is based on the response of these anatomical regions to dose of irradiation, future studies will have to investigate larger cohorts across several dose regimens to parse out the interaction of dose and brain area on these behavioral abilities. Further, functional endpoints (e.g., behaving animal recordings) and direct neurotransmitter evaluation (e.g. microdialysis) will need to be used both before and after irradiation to elucidate the contribution of these separate brain areas to the fWBI induced cognitive impairment.

In conclusion, translation of a fractionated clinical paradigm into rodents is difficult and several well designed dose-response studies with multiple behavioral outcomes are required to facilitate model development to achieve physiological and behavioral end points comparable to the clinical experience.

Acknowledgments

The authors would like to thank Dr. Craig Ferris for his collegiality and resource sharing.

This work was funded by a NIH Grant CA119990 to JBB. Additional personnel support was provided by NIH Grant CA112593 to MER, Department of Radiation Oncology and the Dalton McMichael Fund in Cancer Research.

References

American Cancer Society. Cancer Facts & Figures. Vol. 2014. Atlanta, Georgia, USA: American Cancer Society; 2014.

Belka C, Budach W, Kortmann RD, Bamberg M. Radiation induced CNS toxicity – molecular and cellular mechanisms. Br J Cancer. 2001; 85:1233–1239. [PubMed: 11720454]

Chabert S, Scifo P. Diffusion signal in magnetic resonance imaging: origin and interpretation in neurosciences. Biol Res. 2007; 40:385–400. [PubMed: 18575674]

Chan KC, Khong PL, Cheung MM, Wang S, Cai KX, Wu EX. MRI of late microstructural and metabolic alterations in radiation-induced brain injuries. J Magn Reson Imaging. 2009; 29:1013–1020. [PubMed: 19388094]

Cools R. Dopaminergic modulation of cognitive function-implications for l-DOPA treatment in Parkinson's disease. Neuroscience & Biobehavioral Reviews. 2006; 30:1–23. [PubMed: 15935475]

Dellani PR, Eder S, Gawehn J, Vucurevic G, Fellgiebel A, Muller MJ, Schmidberger H, Stoeter P, Gutjahr P. Late structural alterations of cerebral white matter in long-term survivors of childhood leukemia. J Magn Reson Imaging. 2008; 27:1250–1255. [PubMed: 18504742]

Ferris CF, Kulkarni P, Sullivan JM, Harder JA, Messenger TL, Febo M. Pup Suckling Is More Rewarding Than Cocaine: Evidence from Functional Magnetic Resonance Imaging and Three-Dimensional Computational Analysis. The Journal of Neuroscience. 2005; 25:149–156. [PubMed: 15634776]

Fletcher GH. Hypofractionation: lessons from complications. Radiother Oncol. 1991; 20:10–15. [PubMed: 2020750]

Forbes ME, Paitsel M, Bourland JD, Riddle DR. Systemic effects of fractionated, whole-brain irradiation in young adult and aging rats. Radiat Res. 2013; 180:326–333. [PubMed: 23952575]

Gaber MW, Sabek OM, Fukatso K, Wilcox HG, Kiani MF, Merchant TE. Differences in ICAM-1 and TNF-alpha expression between large single fraction and fractionated irradiation in mouse brain. Int J Radiat Biol. 2003; 79:359–366. [PubMed: 12943244]

Greene-Schloesser D, Robbins ME, Peiffer AM, Shaw EG, Wheeler KT, Chan MD. Radiation-induced brain injury: A review. Front Oncol. 2012; 2:73. [PubMed: 22833841]

Hafty, BG.; Wilson, LD. Handbook of Radiation Oncology: Basic Principles and Clinical Protocols. Boston, Massachusetts, USA: Jones and Bartlett; 2007.

Harrop JP, Dean JA, Paskett ED. Cancer Survivorship Research: A Review of the Literature and Summary of Current NCI-Designated Cancer Center Projects. Cancer Epidemiology Biomarkers & Prevention. 2011; 20:2042–2047.

Jemal A, Bray F, Center MM, Ferlay J, Ward E, Forman D. Global cancer statistics. CA: A Cancer Journal for Clinicians. 2011; 61:69–90. [PubMed: 21296855]

Khong PL, Leung LH, Fung AS, Fong DY, Qiu D, Kwong DL, Ooi GC, Mcalonon G, Cao G, Chan GC. White matter anisotropy in post-treatment childhood cancer survivors: preliminary evidence of association with neurocognitive function. J Clin Oncol. 2006; 24:884–890. [PubMed: 16484697]

Kolb B, Mychasiuk R, Muhammad A, Li Y, Frost DO, Gibb R. Experience and the developing prefrontal cortex. Proceedings of the National Academy of Sciences. 2012; 109:17186–17193.

Landier W, Bhatia S, Eshelman DA, Forte KJ, Sweeney T, Hester AL, Darling J, Armstrong FD, Blatt J, Constine LS, Freeman CR, Friedman DL, Green DM, Marina N, Meadows AT, Neglia JP, Oeffinger KC, Robinson LL, Ruccione KS, Sklar CA, Hudson MM. Development of Risk-Based Guidelines for Pediatric Cancer Survivors: The Children's Oncology Group Long-Term Follow-Up Guidelines From the Children's Oncology Group Late Effects Committee and Nursing Discipline. Journal of Clinical Oncology. 2004; 22:4979–4990. [PubMed: 15576413]

Molina DP, Ariwodola OJ, Weiner JL, Brunso-Bechtold JK, Adams MM. Growth hormone and insulin-like growth factor-I alter hippocampal excitatory synaptic transmission in young and old rats. Age (Dordr). 2013; 35:1575–1587. [PubMed: 22851280]

Moustafa AA, Gluck MA. Computational cognitive models of prefrontal-striatal-hippocampal interactions in Parkinson’s disease and schizophrenia. Neural Networks. 2011; 24:575–591. [PubMed: 21411277]

Peiffer AM, Shi L, Olson J, Brunso-Bechtold JK. Differential effects of radiation and age on diffusion tensor imaging in rats. Brain Res. 2010; 1351:23–31. [PubMed: 20599817]

Pierpaoli C, Jezzard P, Basser PJ, Barnett A, Di Chiro G. Diffusion tensor MR imaging of the human brain. Radiology. 1996; 201:637–648. [PubMed: 8939209]

Shi L, Adams MM, Long A, Carter CC, Bennett C, Sonntag WE, Nicolle MM, Robbins M, D'Agostino R, Brunso-Bechtold JK. Spatial learning and memory deficits after whole-brain irradiation are associated with changes in NMDA receptor subunits in the hippocampus. Radiat Res. 2006; 166:892–899. [PubMed: 17149974]

Shi L, Linville MC, Iversen E, Molina DP, Yester J, Wheeler KT, Robbins ME, Brunso-Bechtold JK. Maintenance of white matter integrity in a rat model of radiation-induced cognitive impairment. J Neurol Sci. 2009; 285:178–184. [PubMed: 19625028]

Shi L, Molina DP, Robbins ME, Wheeler KT, Brunso-Bechtold JK. Hippocampal neuron number is unchanged 1 year after fractionated whole-brain irradiation at middle age. Int J Radiat Oncol Biol Phys. 2008; 71:526–532. [PubMed: 18474312]

Sotak CH. The role of diffusion tensor imaging in the evaluation of ischemic brain injury - a review. NMR Biomed. 2002; 15:561–569. [PubMed: 12489102]

Von Der Weid NX. Adult life after surviving lymphoma in childhood. Support Care Cancer. 2008; 16:339–345. [PubMed: 18196290]

Wang S, Wu EX, Qiu D, Leung LH, Lau HF, Khong PL. Longitudinal diffusion tensor magnetic resonance imaging study of radiation-induced white matter damage in a rat model. Cancer Res. 2009; 69:1190–1198. [PubMed: 19155304]

Yuan H, Gaber MW, Boyd K, Wilson CM, Kiani MF, Merchant TE. Effects of fractionated radiation on the brain vasculature in a murine model: blood-brain barrier permeability, astrocyte

proliferation, and ultrastructural changes. Int J Radiat Oncol Biol Phys. 2006; 66:860–866. [PubMed: 17011458]

Zhang K, Sejnowski TJ. A universal scaling law between gray matter and white matter of cerebral cortex. Proceedings of the National Academy of Sciences. 2000; 97:5621–5626.

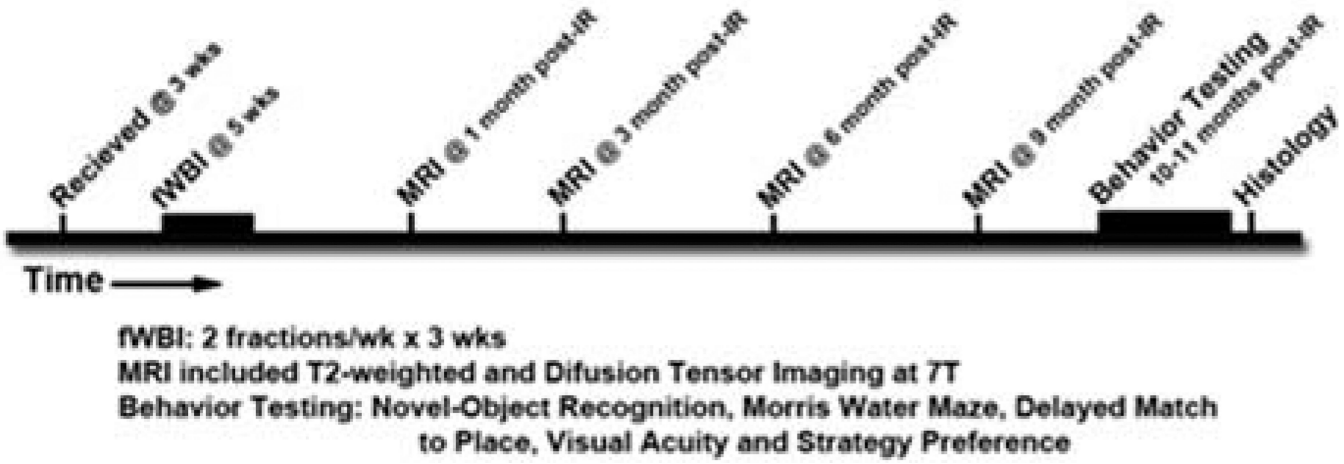

Figure 1.
Study Timeline from receipt of animals to Histology.

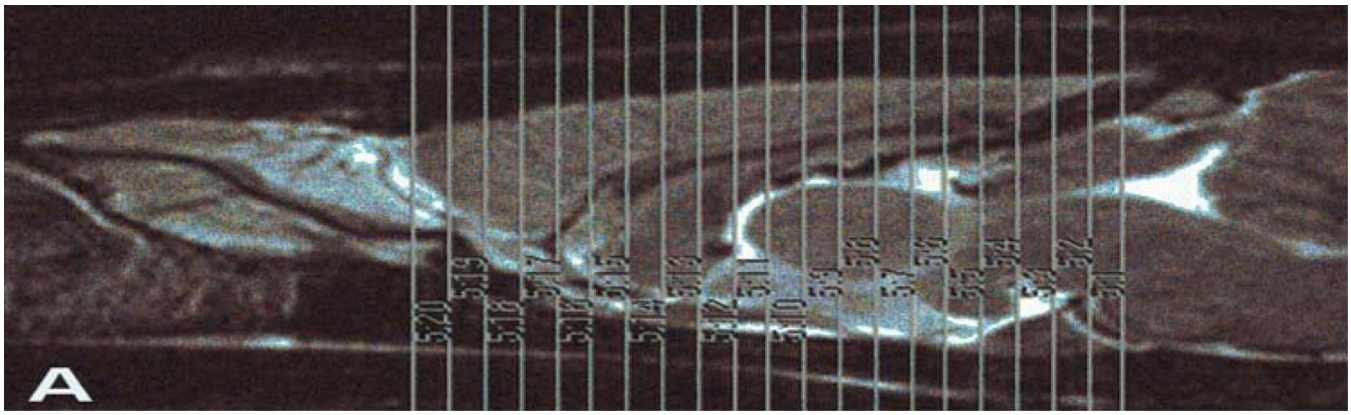

Figure 2.

Part A- T2 scan illustrating slice (n=20) placement for DTI analysis. Slices are 0.62mm thick. Part B- Anatomic ROI atlas overlaid onto an example λ1 image following registration. White bar in upper left of image equals 1mm.

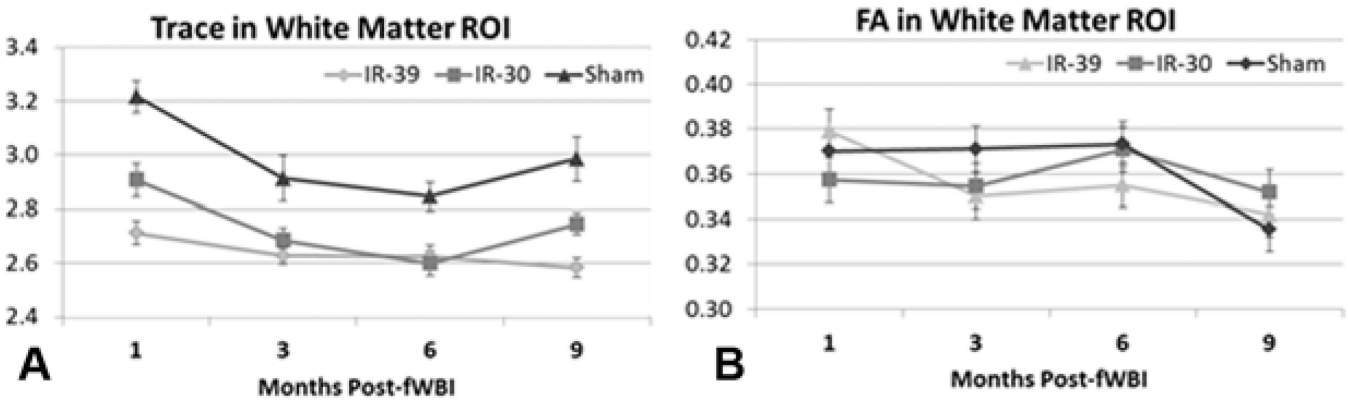

Figure 3.

Part A- Trace values for the white matter ROI for all imaging time points. A significant main effect of reduced diffusion is seen for IR-30 and IR-39 animals relative to sham rats. Part B- Fractional Anisotropy (FA) values, however, did not show any significant group differences and remained essentially the same across the imaging time points. In rats, it does not appear that an fWBI dose of 30 or 39Gy causes significantly measurable white matter breakdown as seen in adult survivors of childhood cancer. Error bars indicate the standard error of the mean (SEM).

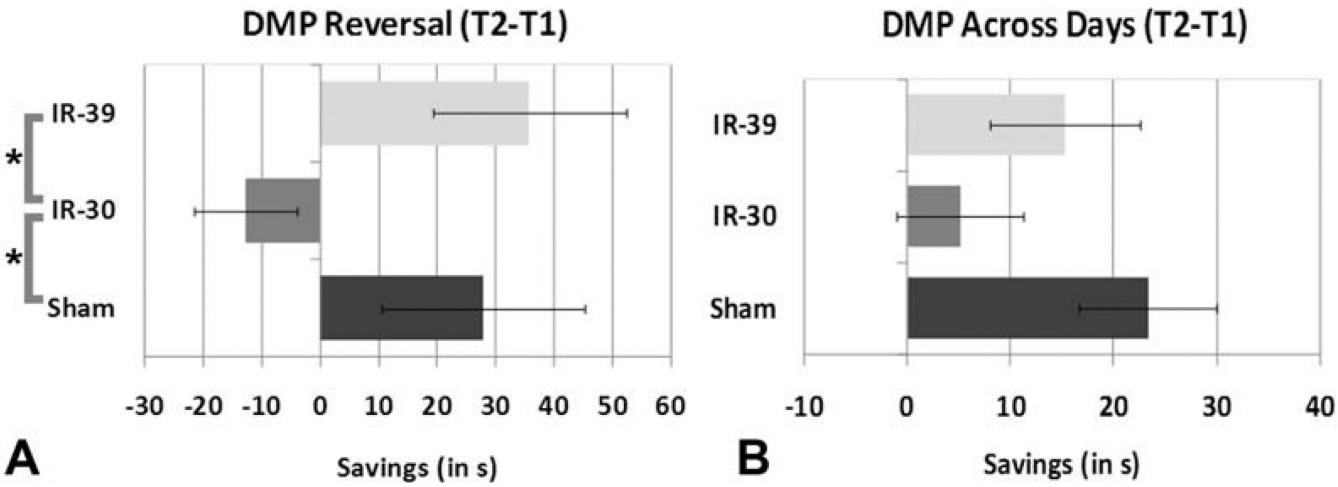

Figure 4.

Part A- Reversal data of Day 1 savings with Sham and IR-39 both performing better than IR-30 rats (*$p<0.05$). While the trend for this remained over the 4 days of DMP testing (part B), results were no longer significantly different. The difference between Sham and IR-30 rats was marginally significant ($p<0.06$) while the difference between IR-30 and IR-39 was not ($p<0.16$). Error bars indicate the standard error of the mean (SEM).

Table I

Probe 1 Preference results for each animal

Preferred Strategy	Sham	IR-30*	IR-39
Place (hippocampal dependent)	5	2	5
Cue (striatal mediated)	4	8	5

*$p<0.06$ for χ^2 distribution analysis